RSC Advances

PAPER

View Article Online
View Journal | View Issue

Cite this: *RSC Adv.*, 2015, **5**, 43765

Highly efficient electromagnetic interference shielding using graphite nanoplatelet/poly(3,4-ethylenedioxythiophene)–poly(styrenesulfonate) composites with enhanced thermal conductivity†

Nidhi Agnihotri,[a] Kuntal Chakrabarti‡*[b] and Amitabha De*[a]

Received 2nd December 2014
Accepted 16th April 2015

DOI: 10.1039/c4ra15674a

www.rsc.org/advances

Graphite nanoplatelet (GNP)/conducting polymer (poly(3,4-ethylenedioxythiophene)–poly(styrenesulfonate)) (PEDOT:PSS) composites were synthesized to evaluate their electromagnetic interference (EMI) shielding effectiveness (SE) in the X-band frequency region. The use of a conducting polymer, instead of a conventional polymer, as the base matrix for the composite negates the primary requirement of achieving the percolation threshold to get an appreciable SE. We show that an addition of 0.5 wt% GNPs to PEDOT:PSS takes the EMI SE to ~30 dB. For 10 and 25 wt% GNP loadings the SE, with dominant absorption, reaches the value of ~47 and 70 dB, respectively, for a thickness of 0.8 mm. The SE remains nearly constant for the whole frequency range and is the highest achieved so far for non-porous, non-foamy carbon composites of comparable thickness. Owing to their low density, GNP/PEDOT:PSS composites give a high specific EMI SE of up to 67.3 dB cm^3 g^{-1}, which is higher compared to even foam structures particularly designed for making low density EMI shields. The drawbacks of foam structures like brittleness and crack formation could also be avoided. Addition of GNPs to PEDOT:PSS results in a several times increase in its pristine thermal conductivity, making it capable of long term use by reducing the chances of chemical degradation through the formation of hot-spots.

Introduction

The rapid penetration of modern electronics into every sphere of our lives has come with the cost of increased electromagnetic interference (EMI). EMI, consisting of spurious radiation signals of electrical origin, causes serious degradation of the performance and reliability of electrical instruments. Shielding plays the crucial role of protecting equipment otherwise susceptible to EMI. Therefore, great effort has been devoted to developing effective EMI shielding materials.

EMI shielding effectiveness (EMI SE), defined as the logarithmic ratio of transmitted power to incident power, depends on a number of physical properties of the shielding material, like the electrical conductivity (σ) (*i.e.* on mobile charge carriers) and the dielectric constant (ε_r). The principal mechanisms of shielding are reflection and absorption. In the case of reflection of radiation, mobile charges like electrons interact with the incident electromagnetic field.[1] Metals typically show this type of shielding. Whereas, when the electrical (or magnetic) dipoles of a highly dielectric material (or a material with a high magnetic permeability) interact with the incident radiation significant absorption takes place.[1] Another mechanism of shielding relies on multiple reflections at the various surfaces or interfaces in the shielding material and this is how composites containing polymers and electrically conducting fillers work.

Unlike metals, which are usually rigid, prone to corrosion and impose a severe weight penalty, electrically conducting polymer composites (CPC) offer several distinct advantages like light weight, flexibility, resistance to corrosion, tunable conductivity and comparatively lower cost than metals.[2–4] These advantages make them particularly suitable for aerospace and mobile applications.

Recent trends to explore the shielding properties of polymer/non-metallic composites have led to the use of different types of combinations of the same by researchers. For example, Yong Li *et al.* studied multiwalled carbon nanotube (MWCNT) filled polyacrylate composite films,[5] whereas Kim *et al.* explored MWCNT/poly(methylmethacrylate) (PMMA).[6] MWCNTs have also been used with other polymers like polystyrene,[2] fluorocarbon foam *etc.*[7] Other forms of carbon that have been used as a conductive filler for making composite materials for EMI

[a]*Chemical Sciences Division, Saha Institute of Nuclear Physics, 1/AF, Bidhannagar, Kolkata 700064, India. E-mail: amitabha.de@saha.ac.in*

[b]*Kalpana Chawla Centre for Space and Nano Sciences, 3F, Swamiji Nagar, Kolkata 700030, India. E-mail: kchakrabarti@outlook.com*

† Electronic supplementary information (ESI) available. See DOI: 10.1039/c4ra15674a

‡ Currently with Mukesh Patel School of Technology Management and Engineering, SVKM's NMIMS, Vile Parle (W), Mumbai 400056, India.

shielding include single walled carbon nanotubes (SWCNT),[8] carbon fibers,[9] carbon nanofibers,[10] and graphene.[3,11,12]

In the case of composites, the polymers used are mostly of low conductivity and the conductivity depends strongly on the percolating network formed by the filler particles. According to the percolation theory, conductive fillers with high aspect ratios lower the percolation threshold (*i.e.* the minimum percentage of filler required for appreciable conductivity) and, thereby, the critical concentration to achieve the desired EMI SE also comes down.[2] In this context, carbon nanotubes, nanofibers and graphene, all having a large aspect ratio, allow low loading of the filler without compromising the other inherent properties of the polymer.[10] In addition, because of their superior mechanical properties, carbon nanotubes and graphene also provide physical strength to the composite. When the EMI shield is designed to work at high frequencies, the depth of penetration of the electromagnetic radiation is very small and the skin depth (δ), defined as the depth at which the field drops to $1/e$ times the value of the incident radiation, is given by $\delta = (2/\sigma\mu f)^{1/2}$ where f, μ and σ denote frequency, permeability and electrical conductivity, respectively.[2] Both CNTs and graphene (along with related graphene based materials like few- and multi-layered graphene, graphite nanoplatelets (GNP) or nanoflakes (GNF), graphene nanoribbons *etc.*) with their large conductivity and very small dimensions can, therefore, play the key role as efficient fillers in CPC EMI shielding materials. The available data from the literature show that about 8 wt% MWCNTs,[5] or 15 wt% SWCNTs[13] or graphene[11] is needed to obtain an EMI SE of about 20 dB. This is good enough for everyday FCC Class B commercial applications. But for defense purposes a more efficient shielding (>70 dB) is required. However, the additional loading of carbon based fillers beyond a certain percentage is untenable because of processibility problems arising out of poor filler–matrix bonding and severe agglomeration.[3]

In order to reduce the density of the carbon containing polymer composites, foam structures of the same have been made.[2–4,12] However, as mentioned by several groups, during the foaming process the conducting network in the composite becomes impaired.[3,12] Furthermore, the large pores present in the foams make them brittle and often cracks start to evolve. In addition, porous structures are prone to attracting moisture and are susceptible to environmental changes. This causes a serious reliability problem, particularly for outdoor applications in countries with large rainfall or snowfall. It is, therefore, of tremendous technological importance to make a CPC that will have the advantages of high conductivity and lightweight, and yet get rid of the problems resulting from the porosity of the foam structures. The aim of this paper is to address this open issue.

The objective of our present investigation is, therefore, to find a non-foamy CPC with low density and a very high EMI SE. Herein, we report the electromagnetic shielding performances of graphite nanoplatelet (GNP)/conducting polymer composites in the X-band frequency region (8.2–12.4 GHz) to demonstrate that they satisfy both the desired criteria. GNPs are stacks of multilayered graphene sheets with platelet morphology. They are cheaper and easier to produce on a large scale compared to graphene and carbon nanotubes, and because of their very high surface energy form strong interfacial bonds with the host matrix.[14] In addition, composites with GNPs have shown higher thermal conductivity enhancement than with SWCNTs.[15] On the other hand, the use of a conducting polymer, instead of a conventional polymer, as the host matrix of the composite offers a unique advantage that, as it is already in a conducting state, the preliminary requirement to achieve the minimum conductivity (*i.e.*, in other words, the percolation threshold) to get an appreciable SE is negated. The addition of any amount of conducting filler like GNPs would increase the conductivity and thereby a much improved SE with a low filler loading is expected. We have chosen poly(3,4-ethylenedioxythiophene) (PEDOT), with poly(styrenesulfonate) (PSS) as the dopant anion, as the conducting polymer for preparing composites with GNPs. Henceforth it will be referred as PEDOT:PSS. The choice of PEDOT:PSS is justified by its several outstanding properties like high conductivity, ability to spin coat, optical transparency and stability.[16,17] Here we show that the GNP/PEDOT:PSS composite not only exhibits much enhanced SE at a lower thickness and filler percentage, but that its specific shielding effectiveness (*i.e.* SE/density) is far better than any known solid, non-foamy material of comparable thickness.

Experimental

The GNP/PEDOT:PSS samples were prepared using GNPs (lateral dimension ~ 400–800 nm, thickness ~ 15–25 nm, carbon content > 99.5%) and PEDOT:PSS *via* a chemical synthesis route, the details of which are given below.

Materials

Graphite nanoplatelets (code KNG-150), obtained from Xiamen Knano Graphite Technology Co. Ltd. China, were subjected to ultracentrifugation in water–alcohol (isopropyl) medium (10 000 rpm for about an hour) in order to discard the heavier and larger GNPs and to obtain lighter and smaller ones. The quality and reproducibility of the obtained GNPs were checked by Raman spectroscopy, TEM, SEM, and density measurements. It has been found that the GNPs have a lateral dimension of ~400–800 nm, thickness of ~15 nm, carbon content > 99.5% and density of ~2.1 g cm^{-3}. The 3,4-ethylenedioxythiophene (EDOT) monomer and PSS were supplied by Sigma-Aldrich. Ammonium peroxydisulphate (APS) was purchased from Merck. Deionised water from a Millipore Milli-Q ultra-purification system, having a resistivity of 18.2 MΩ cm at 25 °C, was used in sample preparation. EDOT was distilled prior to use. Apart from that, all the chemicals were reagent grade and used as received without further purification.

Synthesis of the GNP/PEDOT:PSS composite

The GNP/PEDOT:PSS composites were prepared by *in situ* polymerization of EDOT monomers in the presence of an appropriate amount of GNPs. An aqueous micellar dispersion was prepared with 1 g PSS in 80 ml of deionized water under constant stirring. To this solution, a corresponding amount of

GNPs (for 0.5, 1, 5, 10 and 25 wt% loadings) and 0.71 g of distilled EDOT monomer (in 1 : 1 mole ratio with respect to PSS) were added and solubilized under constant stirring for 1 h. 1.14 g of APS, in a 1 : 1 mole ratio with the monomer, was added to this mixture as an oxidant. The polymerization reaction was allowed to continue for 20 h under vigorous stirring. The resulting dark blue colored sample remained in the dispersed phase. In order to isolate the sample in the solid state, precipitation was carried out using ethanol as a non-solvent. The precipitate was washed with a copious amount of alcohol–water mixture and dried under vacuum for 24 h at 60 °C. Finally the composite was mold pressed in a specially designed rectangular mold corresponding to the dimensions of the wave guide (1.03 cm × 2.31 cm) sample holder. Another sample containing pristine PEDOT:PSS (*i.e.* without any GNPs) was also prepared to serve as a reference. The resulting samples were 0.8 mm thick [*i.e.* the dimensions of each sample used in this investigation are 10.3 mm × 23.1 mm × 0.8 mm].

Characterization

The morphology of the GNP/PEDOT:PSS composite was investigated using scanning electron microscopy (FEI, Quanta 200) and transmission electron microscopy (FEI Tecnai S-Twin). The room temperature electrical conductivities of the samples were measured by a four probe method using Keithley 2400 as the current source and Keithley 2182A as the voltmeter. The composite samples, mold pressed with the same pressure and conditions as that for preparing samples for EMI SE measurement, were cut into a bar shape (10 mm × 2 mm × 0.8 mm) and four equidistant leads of copper wire, with a width of 1.0 mm, length of 2.0 mm and inter-contact distance of 1.5 mm, were attached to each sample along its length using conductive silver paint as an adhesive for the electrical measurements. Raman spectra were recorded using a Renishaw inVia spectrometer, with a 514.5 nm Ar ion laser. Thermal conductivity was measured with a physical property measurement system (Quantum Design, PPMS Model 6000). For the thermal conductivity measurements we used cylindrical samples with a cross sectional area of ~9.2 mm^2 and length of ~1.5 mm, and followed the "two thermometer-one heater" method (*i.e.* a resistor heater heats one end of the sample and the heat flows through the sample to the other end which is thermally grounded) using a custom-built stage designed for PPMS Model 6000 (Quantum design), the details of which can be found elsewhere.[18] 'Silver epoxy' glue was used to attach gold coated oxygen-free copper contact strips at the ends of the cylindrical samples. The room temperature EMI SE was estimated from the measurement of two port *S*-parameters using a Vector Network Analyzer (VNA) (Agilent Technology E8363B) in the X band frequency range (8.2 to 12.4 GHz). The VNA was calibrated prior to each measurement sequence to minimize error. The sample was placed into the sample holder, which was then fitted into the rectangular wave guide of the appropriate dimensions needed for X-band measurements (1.03 cm × 2.31 cm). Once fitted, the sample completely filled the rectangular opening of the wave guide (Fig. S1†). For each filler-concentration, the measurements were taken five times, and the average results are reported. The standard deviations of the 101 data points are included with the EMI SE data in Table 1.

The measured scattering parameters were S_{11} (the forward reflection co-efficient), S_{21} (the forward transmission co-efficient), S_{12} (the reverse transmission co-efficient) and S_{22} (the reverse reflection co-efficient). The unit for the *S* parameters is decibels (dB).

Results and discussion

Fig. 1a and b show the morphology of the GNPs and GNP/PEDOT:PSS composite, respectively, as found by scanning electron microscopy. High resolution transmission electron micrographs (Fig. 1c and d) reveal that the GNPs (with lateral dimension ~ 800 nm and thickness ~ 15 nm) are well dispersed in the polymer matrix and no large agglomerations can be observed. Furthermore, the PEDOT:PSS chains are uniformly segmented between the GNPs.

Raman spectra of the GNPs, PEDOT:PSS, and the GNP/PEDOT:PSS composite are shown in Fig. 1e. The most prominent peaks in the Raman spectrum of the GNPs are the G-band at ~1580 cm^{-1}, the 2D band at ~2680 cm^{-1}, and the small disorder induced D band at ~1350 cm^{-1}. In the case of the PEDOT:PSS sample, prominent Raman peaks corresponding to $C_\alpha{=}C_\beta(-O)$ stretching (1425 cm^{-1}), C_β–C_β stretching (1368 cm^{-1}) and C_α–C_α inter-ring stretching (1260 cm^{-1}) are clearly visible. The Raman spectrum of the composite shows that both the features of the GNPs and PEDOT:PSS are retained. The values for the density, room temperature electrical conductivity and thermal conductivity of the samples are given in Table 1.

The low density of the GNP/PEDOT:PSS samples can be attributed to the presence of interlayer voids and cavities between the polymer coated GNPs and segmented polymer chains. However, it is worth noting here from Fig. 1a and b that these voids or cavities are much smaller than the regular and dense microcellular cells seen in nanocomposite foams that are reported to have diameters from ~5 μm (ref. 12) up to ~100 μm.[19] Also it is evident from Table 1 that with the increase in GNP content the density as well as the electrical conductivity increase. The samples used here are homogeneous in nature (with less than 0.75% density variation among the various parts of the sample (Table S1†)), so we can infer that the majority of the mass that contributes to the increase in density (which is also a conductor) is well distributed throughout the sample, rather than concentrated at a small portion within it. Again, since the filler GNPs are of a high aspect ratio, the presence of more GNPs will contribute to the larger number of backbone structures for charge transport (because of a similar reason, the high aspect ratio fillers lower the percolation threshold in the conductor–insulator matrix). The presence of conducting fillers in close vicinity also increases the tunnelling probability of the charge carriers.[20] Based on the above argument we can conclude that in this particular set of experiments the enhancement of conductivity with the increase in the GNP filler amount is due to the increase in the number of paths available for charge transport. The synergetic effect is the enhancement in electrical

Table 1 Physical properties of the prepared GNP/PEDOT:PSS composites. Numbers in parentheses show the standard deviation of EMI SE

Sample no.	GNP content (wt%/vol%)	Density (g cm^{-3})	Electrical conductivity (S cm^{-1})	EMI SE (dB)	Thermal conductivity (W m^{-1} K^{-1})
1	0/0	1.011 ± 0.03	1.45 ± 0.04	21 (1.4)	0.19 ± 0.03
2	0.5/0.25	1.019 ± 0.04	1.49 ± 0.05	30 (1.6)	—
3	1.0/0.52	1.023 ± 0.05	1.73 ± 0.05	36 (2.0)	—
4	5.0/2.6	1.026 ± 0.04	2.50 ± 0.04	43 (2.6)	—
5	10.0/4.9	1.031 ± 0.05	3.15 ± 0.05	47 (3.1)	0.60 ± 0.04
6	25.0/12.9	1.041 ± 0.03	6.84 ± 0.06	70 (4.2)	0.83 ± 0.05

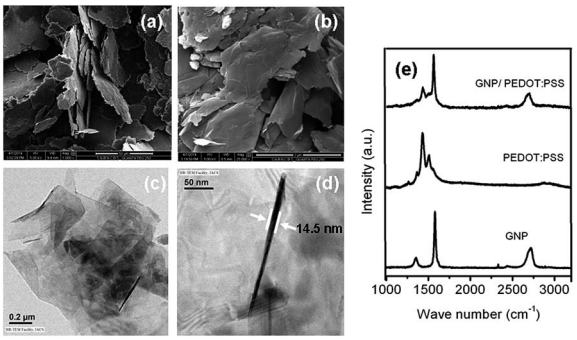

Fig. 1 Scanning electron micrographs of the GNPs (a) and GNP/PEDOT:PSS composite (b). (c and d) Transmission electron micrographs of a GNP/PEDOT:PSS composite with 10% GNPs. (d) reveals that the thickness of the GNPs is ~15 nm. (e) Raman spectra of the GNPs, PEDOT:PSS and the GNP/PEDOT:PSS composite with 10 wt% GNPs.

conductivity and, as a consequence of this, improved SE as discussed in the following sections.

The EMI SE reported in this paper is equivalent to the attenuation in forward transmission of the radiation and is given by $|S_{21}|$. The low (~1%) discrepancies between the forward and reverse measurements confirm the same SE on both sides. Fig. 2 shows the variation of the EMI SE over the frequency range of 8.2–12.4 GHz for GNP/PEDOT:PSS composites with various GNP loadings. The same plot for the pristine PEDOT:PSS sample is also shown.

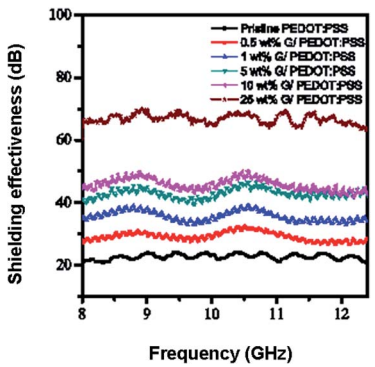

Fig. 2 EMI shielding effectiveness as a function of frequency for the GNP/PEDOT:PSS composites with various GNP loadings.

The pristine PEDOT:PSS without any GNPs gives an EMI SE of about 21 dB. This is obviously quite high compared to the conventional polymer matrices used for carbon based composites, *viz.* polystyrene (<1 dB),[2] poly(dimethylsiloxane) (PDMS) (~1 dB)[3] *etc.*, and comparable to conducting polymers like a polypyrrole impregnated polyurethane membrane (~20 dB).[21] An addition of 0.5 wt% GNPs to PEDOT:PSS increases the EMI SE to ~30 dB. For 10 and 25 wt% GNP loadings the SE reaches a value of about 47 and 70 dB, respectively. It is worth noting here that this is much better than previously reported values of X-band SE and, to the best of our knowledge, the highest value obtained for carbon based composites of comparable thickness. For example, a 7 wt% CNT/polystyrene foam showed a SE of ~ 19 dB for a thickness of 1.2 mm,[2] for 0.8 wt% graphene/PDMS (1 mm thick foam) the SE is 30 dB,[3] and 1.8 vol% graphene/polymethylmethcrylate (2.4 mm thick foam) gives a SE of 19 dB.[12] Even the SE of other combinations, *viz.* 15 wt% graphene/epoxy (21 dB),[11] 30 wt% graphene/polystyrene (29 dB, 2.5 mm),[4] 40 vol% carbon fiber/polyethersulphone (PES) (30–38 dB, 2.87 mm),[9] remains lower than the values reported here. A comparative survey of the SE of various carbon (CNTs/graphene/fibers) containing composites, along with the present results, is given in Table 2.

Yang and co-workers pointed out that for application of EMI shielding in aerospace technology it would be more appropriate to compare different shielding materials in terms of their specific EMI shielding effectiveness (*i.e.* EMI SE/density).[2] For example, nickel has a specific EMI SE of 9.2 dB cm^3 g^{-1} and for copper the same is 10 dB cm^3 g^{-1}.[22] In the present work, the specific EMI SE for the sample with a 0.5 wt% GNP loading is 29.44 dB cm^3 g^{-1}. Whereas, for the samples with 10 and 25 wt% GNP loadings the specific EMI SE is 45.58 and 67.3 dB cm^3 g^{-1}, respectively. Clearly the EMI SE values of the GNP/PEDOT:PSS composites are much higher than those of typical metal shields. They are even better than a CNT/polystyrene composite foam (33.1 dB cm^3 g^{-1}, 1.2 mm thick),[2] 1.8 vol% graphene/PMMA foam (17–25 dB cm^3 g^{-1}, 2.4 mm thick),[12] and 30 wt% graphene/polystyrene composite in porous form (64.4 dB cm^3 g^{-1}, 2.5 mm thick)[4] in the same frequency band. Notably this was achieved avoiding the drawbacks of the porous foams like brittleness and proneness to cracking.

Here we would like to point out that the comparison of different shielding materials in terms of specific EMI SE without the mention of thickness bears no meaning. For example, it has been found that EMI SE is enhanced with increasing thickness

Table 2 EMI shielding effectiveness of different carbon containing composites. Values for copper are also given for comparison

Materials	Filler %	EMI SE (dB)	Specific EMI SE (dB cm^3 g^{-1})	Thickness (mm)	Ref.
Graphene/PEDOT:PSS	0.5 wt%	30	29.4	0.8	Present work
	10 wt%	46	45.6	0.8	
	25 wt%	70	67.3	0.8	
MWCNT/polyacrylate	10 wt%	20	—	1.5	5
MWCNT/fluorocarbon foam	12 wt%	42–48	—	3.8	7
SWCNT/PS foam	7 wt%	19	33	1.2	2
SWCNT/epoxy	15 wt%	15–49	—	1.5	15
Carbon fiber/PES	40 vol%	30–38	—	2.9	9
CDG/PMMA foam	5 wt%	19	17–25	2.4	12
Graphene/PVDF foam	7 wt%	28	—	—	23
Porous graphene/polystyrene	30 wt%	29	64.4	2.5	4
Graphene/PDMS foam	0.8 wt%	30	333	1.0	3
Copper		90	10	3.1	22

of the shielding material.[3] Therefore, the same material with uniform density and composition will give a higher SE, and consequently a better specific EMI SE, when a thicker sample is used for shielding measurements instead of a thinner one. We, therefore propose to compare the efficiency of different shielding materials by specific EMI SE per unit thickness. 1 mm is a good scale for specific EMI SE comparison. Assuming a linear relationship between SE and thickness for a single piece of homogeneous and isotropic material, the specific SE/thickness for 0.5 wt% graphene/PEDOT:PSS was found to be 41.25 dB cm^3 g^{-1} and for 25 wt% GNP/PEDOT:PSS it is 92.95 dB cm^3 g^{-1}, when both have a thickness of 1 mm.

To elucidate the shielding mechanism of the GNP/PEDOT:PSS composite we have also studied the part of the incident radiation that has been reflected and absorbed. When an electromagnetic wave falls on a material the incident power is divided into reflected power, absorbed power and transmitted power. The corresponding reflectivity (R), absorptivity (A) and transmitivity (T) are related as $R + A + T = 1$. Total shielding effectiveness (SE_{Tot}) is the summation of the effectiveness of all the attenuation mechanisms, *viz.* absorption (SE_A), reflection (SE_R) and multiple reflections (SE_M). Thus, $SE_{Tot} = -10 \log(P_t/P_o) = SE_A + SE_R + SE_M$, where P_t and P_o denote transmitted and incoming power, respectively, $SE_{Tot} = S_{21} = -10 \log_{10} T$, $SE_R = -10 \log_{10}(1 - R)$, and $SE_A = -10 \log_{10}[T/(1 - R)]$. R is related to the forward reflection co-efficient (S_{11}) by $S_{11} = 10 \log_{10} R$.[2] The contribution from multiple reflections is assumed to be negligible when $SE_{Tot} \geq 15$ dB.[13] Fig. 3a shows the plots of SE_{Tot}, SE_A and SE_R of the sample with a 10 wt% GNP loading for the whole frequency range. It is quite clear that the main contribution to shielding comes from the absorbance of the incident electromagnetic waves. The same trend is valid for all the samples with different filler percentages (Fig. 3b, with values at 10 GHz). Absorption dominates even for the shielding behavior of the sample without GNPs (*i.e.* pristine PEDOT:PSS) (Fig. S2 in the ESI†). It is worthwhile to mention here that for composites with other forms of carbon, *viz.* SWCNTs and MWCNTs, the dominant shielding mechanism was found to be reflection.[2,13] However, our results show that for GNP composites the microwave (X-band) reflection is negligibly small compared to that of absorption for the whole frequency range. The contribution due to reflection in the GNP/PEDOT:PSS composite is <5 dB, like other graphene containing composites,[4,12] and remains almost constant for all GNP concentrations (Fig. 3b). Fig. 3b also shows that SE_{Tot} and SE_A both increase with increasing GNP percentage. Therefore, it can be concluded that a major part of the contribution due to reflection comes from the base PEDOT:PSS and when GNP filler is added to it the absorption part increases rapidly. The presence of many GNPs, in the form of large face to face two dimensional structures separated by polymer chains, facilitates multiple reflections of the incident microwave radiation inside the composite and, because of its longer stay, the chance for it to get absorbed through lattice heating increases. This leads to absorption-dominant EMI shielding.

The absorption-dominant shielding offers several advantages over a shielding mechanism where reflection is the major contributor. In spite of the ability to prevent the penetration of radiation beyond the shields, reflection dominated EMI shielding may lead to spurious damage to the components of an electric circuit due to reflection coming either from the shield of the neighboring components or from the electronic housing of the circuits with such an EMI shielding cover.[3,19] As pointed out

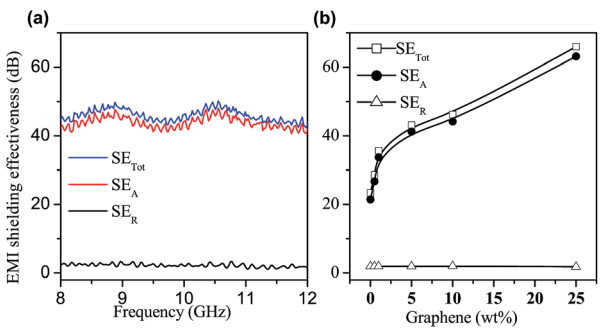

Fig. 3 (a) The comparison between SE_{Tot}, SE_R and SE_A for the graphene/PEDOT:PSS sample with 10% graphene loading, and (b) the same for samples with different graphene loadings at 10 GHz.

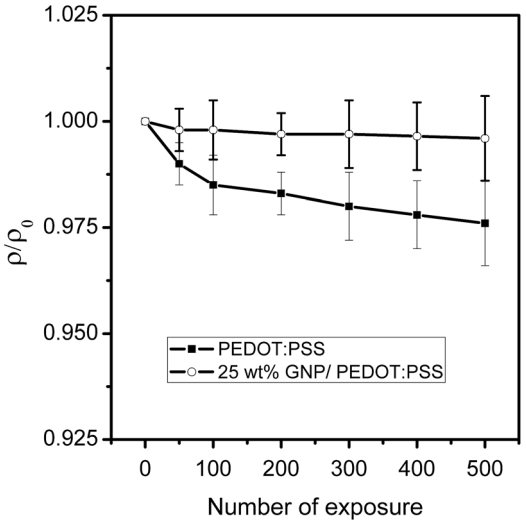

Fig. 4 Resistivity ratio *vs.* number of exposures for the samples with 25 wt% GNPs or pristine PEDOT:PSS. ρ_0 being the initial resistivity.

by Chen *et al.*[3] this type of problem is most perennial when a circuit component, that needs EMI shielding, itself generates EMI radiation. Shielding materials like GNP/PEDOT:PSS, where absorption is the principal shielding mechanism, can get rid of such a problem.

In the case of microwave absorption the material gets heated. Therefore, the thermal behavior of the absorbing material merits special attention. This is particularly important when the absorbing layer is using a polymer as the base material. It is well known that the conventional polymers are poor conductors of heat. As a result, the absorbed energy is often localized and leads to the formation of 'hot-spots' causing irreversible structure degradation.[24] Several groups have studied the thermal degradation of PEDOT:PSS and found that prolonged exposure to high temperature decreases the electrical conductivity of PEDOT:PSS.[25,26] Since EMI SE depends directly on conductivity, it is also expected to decrease. Thus there exists a close relation between the EMI SE and thermal conductivity of the shielding material. However, there is a dearth in EMI literature where the thermal conductivity has been reported for the shielding material. With the advent of graphene and EMI shielding, where absorption is the dominant mechanism, this can no longer be ignored. The room temperature thermal conductivity of pristine PEDOT:PSS was measured and was found to be ~0.19 W m^{-1} K^{-1}, close to the values reported.[27] When GNPs (thermal conductivity ~ 3000 W m^{-1} K^{-1}) are mixed with a polymer, its thermal conductivity is expected to increase. According to a parallel thermal resistor model[27] the thermal conductivity of the composite (k) is given by $k = k_m V_m + k_f V_f$, where k_m and k_f denote the thermal conductivities of the matrix and the filler, respectively, and V_m and V_f are the volume fractions (*i.e.* volume of the indexed material/total volume) of the matrix and the filler. Taking $k_m = 0.2$ W m^{-1} K^{-1}, $k_f = 3000$ W m^{-1} K^{-1} and the densities of the GNPs and polymer as 2.25 and 1 g cm^{-3}, respectively, for 25 wt% graphene loading the theory predicts a thermal conductivity of ~ 250 W m^{-1} K^{-1}. However, it has been found that for 10 wt% GNP/PEDOT:PSS the room temperature thermal conductivity is 0.6 W m^{-1} K^{-1}, whereas when the GNP loading is 25 wt% it becomes 0.83 W m^{-1} K^{-1}. This discrepancy arises due to the fact that nano-inclusions and nanointerfaces act as scattering centers for phonons and thereby reduce the value of thermal conductivity.[28,29] Many of the GNP–GNP junctions are capped by thin layers of PEDOT:PSS and this hinders the phonon (*i.e.* thermal energy) transport through GNP–PEDOT:PSS–GNP interfaces. The thermal conductivity values of the GNP/PEDOT:PSS composites reported here are, however, similar to or better than graphite/epoxy (~0.25 W m^{-1} K^{-1}),[30] MWCNT/epoxy (~0.45 W m^{-1} K^{-1})[30] or SWCNT/PANI (~1.0 W m^{-1} K^{-1})[29] with similar filler loadings. The high thermal conductivity is very important in tandem with the high EMI SE of the graphene based polymer composites, because now the heat can be well distributed throughout the sample. Consequently the energy can be transferred to the environment more efficiently and the chance of hot-spot formation is reduced significantly.

To estimate the thermal degradation behavior of the composites, two samples, one with 25 wt% GNP loading and the reference pristine sample (*i.e.* without any GNPs), were subjected to repeated microwave exposure, 500 times at 40 W power (each exposure time being 180 s). It was found that the resistance of the reference pristine sample showed ~3% decrease from the initial value, whereas for the sample with 25 wt% graphene there was no significant resistance drop (Fig. 4).

Consequently, there has been ~5 dB decline in the SE of the pristine sample. In case of other samples it is, however, less than 1 dB. Therefore, it can be concluded that due to the high thermal conductivity of the GNP/PEDOT:PSS sample it can withstand the thermal degradation and/or the thermal fatigue much better than the pristine PEDOT:PSS sample. Thus the higher thermal conductivity of GNP/PEDOT:PSS than pristine PEDOT:PSS makes it particularly suitable for long term applications as EMI shielding material.

Conclusions

This paper addresses the ongoing quest for high efficiency, lightweight and thermally conducting EMI shields. GNP/PEDOT:PSS composites with different amounts of graphene loading have been prepared. The composites provide a high X-band SE from 30 dB (with 0.5 wt% GNP loading) up to 70 dB (with 25 wt% GNP loading) for a thickness of only 0.8 mm, which surpasses the best reported values of EMI SE for materials with a comparable thickness. The use of a conducting polymer, instead of a conventional polymer, to make the composite eliminates the primary requirement of achieving the percolation threshold and pushes the SE to a higher value with low filler content. Owing to their low density, GNP/PEDOT:PSS composites give high specific EMI SE values, up to a value of 67.3 dB cm^3 g^{-1}. The values are higher compared to even foam structures particularly designed for making low density EMI shields. The negative aspects of foam structures like brittleness and crack formation could also be avoided. The addition of 25 wt% GNPs has increased the thermal conductivity of PEDOT/

PSS by greater than four times that of its pristine value, making it capable of long term use by reducing the chance of chemical degradation through the formation of hot-spots. Equipped with their high thermal conductivity and large EMI SE, the GNP/PEDOT:PSS composites promise efficient shielding for use in mobile, aerospace, defense and electronic industries.

Acknowledgements

Authors thank Nazir Khan, Ajoy Kumar Bhattacharya, Ankan Dutta Chowdhury and Dr Deep Talukdar for helpful discussion. This work is supported by BARD Project, SINP.

References

1 D. D. L. Chung, *Carbon*, 2001, **39**, 279–285.
2 Y. Yang, M. C. Gupta, K. L. Dudley and R. W. Lawrence, *Nano Lett.*, 2005, **5**, 2131–2134.
3 Z. Chen, C. Ma, W. Ren and H. M. Cheng, *Adv. Mater.*, 2013, **25**, 1296–1300.
4 D. X. Yan, P. G. Ren, H. Pang, Q. Fu, M. B. Yang and Z. M. Li, *J. Mater. Chem.*, 2012, **22**, 18772–18774.
5 Y. Li, C. Chen, S. Zhang, Y. Ni and J. Huang, *Appl. Surf. Sci.*, 2008, **254**, 5766–5771.
6 H. M. Kim, K. Kim, C. Y. Lee, J. Joo, S. J. Cho, H. S. Yoon, D. A. Pejakovic, J. W. Yoo and A. J. Epstein, *Appl. Phys. Lett.*, 2004, **84**, 589–591.
7 A. Fletcher, M. C. Gupta, K. L. Dudley and E. Vedeler, *Compos. Sci. Technol.*, 2010, **70**, 953–958.
8 B. Aissa, L. L. Laberghe, M. A. Habib, T. A. Denidni, D. Therriault and M. A. El Khakani, *J. Appl. Phys.*, 2011, **109**, 084313.
9 L. Li and D. D. L. Chung, *Composites*, 1994, **25**, 215–223.
10 Y. Yang, M. C. Gupta, K. L. Dudley and R. W. Lawrence, *Adv. Mater.*, 2005, **17**, 1999–2003.
11 J. J. Liang, Y. Wang, Y. Huang, Y. Ma, Z. Liu, J. Cai, C. Zhang, H. Gao and Y. Chen, *Carbon*, 2009, **47**, 922–925.
12 H. B. Zhang, Q. Yan, W. G. Zheng, Z. He and Z. Z. Yu, *ACS Appl. Mater. Interfaces*, 2011, **3**, 918–924.
13 C. Basavaraja, G. T. Noh and D. S. Huh, *Colloid Polym. Sci.*, 2013, **291**, 2755–2763.
14 A. Yu, P. Ramesh, X. Sun, E. Bekyarova, M. E. Itkis and R. C. Haddon, *Adv. Mater.*, 2008, **20**, 4740–4744.
15 N. Li, Y. Huang, F. Du, X. He, X. Lin, H. Gao, Y. Ma, F. Li, Y. Chen and P. C. Eklund, *Nano Lett.*, 2006, **6**, 1141–1145.
16 A. M. Nardes, M. Kemerink, M. M. deKok, E. Vinken, K. Maturova and R. A. J. Janssen, *Org. Electron.*, 2008, **9**, 727–734.
17 T. Stocker, A. Kohler and R. Moos, *J. Polym. Sci., Part B: Polym. Phys.*, 2012, **50**, 976–982.
18 M. B. Bryning, D. E. Milkie, M. F. Islam, J. M. Kikkawa and A. G. Yodh, *Appl. Phys. Lett.*, 2005, **87**, 161909.
19 J. M. Thomassin, C. Pagnoulle, L. Bednarz, I. Huynen, R. Jerome and D. Detrembleur, *J. Mater. Chem.*, 2008, **18**, 792–796.
20 P. Sheng, E. K. Sichel and J. I. Gittleman, *Phys. Rev. Lett.*, 1978, **40**, 1197–1199.
21 Y. Wang and X. Jing, *Polym. Adv. Technol.*, 2005, **16**, 344–351.
22 X. P. Shui and D. D. L. Chung, *J. Electron. Mater.*, 1997, **26**, 928–934.
23 V. Eswaraiah, V. Sankaranarayanan and R. Ramaprabhu, *Macromol. Mater. Eng.*, 2011, **296**, 894.
24 A. Peacock and A. Calhoun, *Polymer Chemistry: Properties and Applications*, Carl Hanser Verlag, Munich, Germany, 2006.
25 E. Vitoratos, S. Sakkopoulos, N. Paliatsas, K. Emmanouil and S. A. Choulis, *Open J. Org. Polym. Mater.*, 2012, **2**, 7–11.
26 E. Vitoratos, S. Sakkopoulos, E. Dalas, N. Paliatsas, D. Karageorgopoulos, F. Petraki, S. Kennou and S. A. Choulis, *Org. Electron.*, 2009, **10**, 61–66.
27 D. Kim, Y. Kim, K. Choi, J. C. Grunlan and C. Yu, *ACS Nano*, 2010, **4**, 513–523.
28 A. J. Minnich, M. S. Dresselhaus, Z. F. Ren and G. Chen, *Energy Environ. Sci.*, 2009, **2**, 466–479.
29 Q. Yao, L. Chen, W. Zhang, S. Liufu and X. Chen, *ACS Nano*, 2010, **4**, 2445–2451.
30 S. H. Song, K. H. Park, B. H. Kim, Y. W. Choi, G. H. Jun, D. J. Lee, B. S. Kong, K. W. Paik and S. Jeon, *Adv. Mater.*, 2013, **25**, 732–737.